НАУЧНО-ТЕХНИЧЕСКИЙ ВЕСТНИК ИНФОРМАЦИОННЫХ ТЕХНОЛОГИЙ, МЕХАНИКИ И ОПТИКИ
ноябрь–декабрь 2022 Том 22 № 6 http://ntv.ifmo.ru/
SCIENTIFIC AND TECHNICAL JOURNAL OF INFORMATION TECHNOLOGIES, MECHANICS AND OPTICS
November–December 2022 Vol. 22 No 6 http://ntv.ifmo.ru/en/
ISSN 2226-1494 (print) ISSN 2500-0373 (online)

НОВЫЕ МАТЕРИАЛЫ И НАНОТЕХНОЛОГИИ
MATERIAL SCIENCE AND NANOTECHNOLOGIES

doi: 10.17586/2226-1494-2022-22-6-1078-1084

Luminescence technique for studying the growth of $AgInS_2$ quantum dots

Ahmad K. Ahmad[1]✉, Ammar H. Mohammed[2], Alexander A. Skaptsov[3]

[1] Al-Nahrain University, College of Engineering, Baghdad, 10072, Iraq
[2] Al-Nahrain University, College of Science, Baghdad, 10072, Iraq
[3] Saratov State University, Saratov, 410012, Russian Federation

[1] ahmad.ahmad@nahrainuniv.edu.iq✉, https://orcid.org/0000-0003-3522-4701
[2] ammarhussen659@gmail.com, https://orcid.org/0000-0003-3646-4790
[3] skaptsov@yandex.ru, https://orcid.org/0000-0001-9336-6885

Abstract

Although nanoparticle production techniques are well-known, getting nanoparticles with specific characteristics that enable their application as biosensors is an entirely other problem. Many issues occur as a result of employing the method for producing repeatable and time-stable nanostructures. We created $AgInS_2$ nanoparticles as colloidal quantum dots in a variety of methods to test the efficiency of the synthesis process on the optical characteristics of the nanoparticles, as well as their size, composition, absorption, and luminescence spectra. The capillary electrophoresis (CE) approach for $AgInS_2$ production was employed, with modifications in solvent and temperature, to get nanocrystal (NC) particles. The researchers discovered that Ag accumulation in the InS lattice promotes deformation which leads to structural defects. Consequently, the direction of a nanoparticle light band may now be changed. The features of mixed $AgInS_2$ nanoparticles have been examined with respect to different fabrication procedures, surface stability, and metal impurity incorporation. One band dominates in the luminescence spectra of $Ag_xIn_{1-x}S_2$ nanoparticles. The relationship between the stoichiometric ratio, luminescence amplitude, line width, and the maximum wavelength is investigated. The average size of the received nanocrystals was determined using dynamic light scattering studies. The computed nanoparticle diameter range has an average particle size of 3–3.5 nm.

Keywords

$AgInS_2$, quantum dot, luminescence, synthesis of nanocrystalline particles, biosensors

For citation: Ahmad A.K., Mohammed A.H., Skaptsov A.A. Luminescence technique for studying the growth of $AgInS_2$ quantum dots. *Scientific and Technical Journal of Information Technologies, Mechanics and Optics*, 2022, vol. 22, no. 6, pp. 1078–1084. doi: 10.17586/2226-1494-2022-22-6-1078-1084

УДК 535.37:544.77.051

Люминесцентный метод исследования роста квантовых точек $AgInS_2$

Ахмад Карнал Ахмад[1]✉, Аммар Хуссейн Мохаммед[2], Александр Александрович Скапцов[3]

[1] Аль-Нарейн Юниверсити, Инженерный колледж, Багдад, 10072, Ирак
[2] Аль-Нарейн Юниверсити, Багдад, 10072, Ирак
[3] Саратовский национальный исследовательский государственный университет имени Н.Г. Чернышевского, Саратов, 410012, Российская Федерация

[1] ahmad.ahmad@nahrainuniv.edu.iq✉, https://orcid.org/0000-0003-3522-4701
[2] ammarhussen659@gmail.com, https://orcid.org/0000-0003-3646-4790
[3] skaptsov@yandex.ru, https://orcid.org/0000-0001-9336-6885

Аннотация

Методы получения наночастиц хорошо известны, однако стабильно повторяемое получение наночастиц с одинаковыми специфическими характеристиками, позволяющими их использовать в качестве биосенсоров, в настоящее время представляет собой проблему. Проблема многих методов заключается в получении результатов с хорошей воспроизводимостью оптических свойств и их стабильностью во времени. В работе получены

наночастицы $AgInS_2$ в виде коллоидных квантовых точек различными методами. Выполнен анализ процесса синтеза, который влияет на оптические характеристики наночастиц, их размер, состав, спектры поглощения и люминесценции. Для получения нанокристаллических частиц при изготовлении $AgInS_2$ применен капиллярный электрофорез с модификациями растворителя и температуры. Обнаружено, что накопление Ag в решетке InS способствует деформации, которая приводит к структурным дефектам и, следовательно, к смещению спектральной полосы люминесценции. Исследованы характеристики смешанных наночастиц $AgInS_2$ при различных вариациях технологии изготовления, стабильности поверхности и включения металлических примесей. Показано, что в спектрах люминесценции наночастиц $Ag_xIn_{1-x}S_2$ доминирует одна полоса. Исследована зависимость между стехиометрическим соотношением, амплитудой люминесценции, шириной линии и максимальной длиной волны. Средний размер полученных нанокристаллов определен с использованием метода динамического светорассеяния. Расчетный размер наночастиц составил в среднем 3–3,5 нм.

Ключевые слова

$AgInS_2$, квантовые точки, люминесценция, синтез наноструктур, биосенсоры

Ссылка для цитирования: Ахмад А.К., Мохаммед А.Х., Скапцов А.А. Люминесцентный метод исследования роста квантовых точек $AgInS_2$ // Научно-технический вестник информационных технологий, механики и оптики. 2022. Т. 22, № 6. С. 1078–1084 (на англ. яз.). doi: 10.17586/2226-1494-2022-22-6-1078-1084

Introduction

In recent years, $AgInS_2$ nanocrystals have garnered a great deal of interest among semiconductors of groups I, III, and VI due to their various benefits, such as their customizable optical characteristics, high extinction coefficients, high quantum yields, diverse emission spectra, and photochemical durability. Several techniques, mostly based on thermolytic one-of-a-kind metallic-sulfur complexes or direct metallic response cations and sulphur with suitable covering reagents [1, 2], have been published for the ternary synthesis of $AgInS_2$ with varied sizes. Metallic cations are typically coupled with amines or dodecanethiol to form complex metallic precursors, such as Colloidal Quantum Dots (CODs), which offer particles with controlled outgrowth [3]. Sulfur can be derived from elemental sulphur, thiols, dithiocarbamates, or carbon disulfide, all of which are soluble in organic solvents [4, 5]. Metallic thiolates or dithiocarbamates have been used as a source of both metal cations and sulfur [6].

Recently, it has been observed that studies and research focus on the use of CQDs. They are 2–10 nm long semiconductor nanocrystals that blend the physical and chemical properties of molecules with the optoelectronic properties of semiconductors. Quantum dots (QDs) have high fluorescence brightness and are more resistant to picture bleaching than fluorophores making them excellent candidates for long-term study. The author recommended against conjugating CQDs derived from non-toxic $AgInS_2$/ZnS compounds with nanoparticles of other types.

Using novel synthesis techniques and materials, it is possible to increase the quantum yield of QDs significantly. CQDs play a crucial role in the current world, particularly for biomedical applications where they may be used to identify or pinpoint various illnesses and subsequently to provide medicine locally utilizing the same circuit class therapy but with a vaccine medication. In this context, the development of CQD-based labeling for less hazardous semiconductors of groups I-III and VI, such as $CuInS_2$ and $AgInS_2$, appears promising. This form of CQD is distinguished by the ability to tune the emission band from the visible to the near-infrared region and by the comparatively long lifetime of an excited state. This study aims to investigate the feasibility of using $AgInS_2$-based QDs for fluorescence imaging of biological objects and to compare their performance with that of fluorescent dyes immobilized on the surface of nanoparticles.

Indium silver disulfide is a semiconductor that has shown promise in solar photovoltaics [7, 8]. This semiconductor has potential applications in photocells that concentrate solar energy, in cascade structures with a gradient in width, and in noisy zones. The combination of indium disulfide with ribs and, for example, indium di-selenide copper with a common base of CdS can result in a tenfold improvement in efficiency [9, 10]. By matching the crystal lattices of the semiconductors mentioned above, $AgInS_2$ has a high optical absorption (greater than 10^4 cm^{-1}), strong radiation resistance, and low dissipation. Space charge parameters and effective carrier separation may be modified in many multilayer structures, leading to an active investigation of such combinations. $AgInS_2$ bulk crystals and films have received little attention. The goal of this effort is to semi-study $AgInS_2$ films and their electrical, physical, and optical characteristics.

These materials, like $AgInS_2$, are semiconductors belonging to the III group; in the visible and near-ultraviolet spectrum they exhibit enormous gaps range and significant deactivation rates. Because of their luminous qualities, such combinations pique much interest as an alternative for a more dangerous cadmium-containing quantum. Currently, many experiments utilise luminous semiconductors (such as $AgInS_2$) that may be used as Nano thermometers by relying on ambient temperature. As a result, when samples containing $AgInS_2$ nanoparticles (4 nm in size on average) are heated, a drop in fluorescence intensity and spectrum shift is detected concurrently, both under single and two-photon excitation. The connection between fluctuations in the peak wavelength of the radiation is linear with temperature for $AgInS_2$. Currently, luminous nanoparticles are utilized to assess cell temperature in various applications [11, 12]. Laser thermolysis is a significant and promising medical sector, particularly in various operations and treatments.

Photothermolysis employs a variety of photosensitizers, the most effective of which being plasmon-resonant nanoparticles (Plasmon Resonance Nanoparticles) [13, 14]. Due to limited laser radiation absorption when warming the nanoparticles delivered into the tumor

site, laser photothermolysis does little harm to hygiene cells of biological tissue around the tumor. In reality, the fundamental limitation of its efficacy is the problem of unwanted heating of adjacent tissue which also involves normal cells at risk and induces the initiation of coagulation. The heating process must thus be monitored to accomplish biological tissue coagulation in the complete tumor volume and to halt irradiation after disease eradication. Inadequate heating may promote tumor development, while excessive heating may cause healthy biological tissue to clot. As a result, the advancement of the laser photothermolysis process is hampered by a lack of trustworthy or reliable methods for determining optimal exposure settings. Direct and fast detection of thermal fields in organic tissue near Plasmon resonance nanoparticles is feasible for tissue heating control. Several non-invasive thermometry procedures include radiation ultrasound and magnetic resonance imaging.

Despite encouraging results, these approaches are often constrained by their lack of temporal resolution. During photothermolysis, when heating, the biological tissue is specifically marked by non-contact temperature scaling of the surface with a thermal imager or measuring the inside temperature at specific spots with a thermocouple. However, denying the ultimate domination of the heat process interaction and propagation of laser light in tumor materials causes uncertainty in calculating the interior temperature from the obtained surface temperature division with the aforementioned data. As a result, controlled photothermolysis becomes much more challenging. As a result, identifying in real time the spatial distribution of temperature inside biological entities remains crucial. In this scenario, the approach is to create a nanosensor that can forecast the incidence of tissue coagulation that is irreversible. We investigated how temperature affects the luminescence spectra of nanoparticles in aqueous and biological contexts. As the temperature rises, the fluorescence intensity of $AgInS_2$ nanoparticles in water decreases, and a temperature change of 25 °C cause a line shift by 5 nm to the luminescence peak. Furthermore, it was evident that the location of the luminescence peak of $AgInS_2$ nanoparticles is influenced by the medium. By heating the $AgInS_2$ nanoparticles in biological specimens, the peak luminescence shifts linearly to longer wavelengths, where the maximum shear rate is 0.459 ± 0.035 nm.

We created $AgInS_2$ nanoparticles in various methods to assess the influence of the synthesis process on the condition and optical features of nanoparticles, to explore their luminescence spectra, absorption, size, and structure. Colloidal QDs exhibit critical optical properties that are proportional to particle size. Similar to the box model in quantum mechanics, as the border dimensions drop, the energy of each state rises. Subsequent to photon absorption, the valence and conduction hands of the QDs are quantized as a result of the excited state which is an electron-hole pair with dimensions lower than the exciton Bohr radius. This quantization may be demonstrated in QD absorption spectra where discrete low-energy transitions are seen in a clean, monodisperse sample. A particle size function provides the Band edge energy of a QD (E) and is given by the following equation [15]:

$$E = E_g + \left(\frac{\hbar^2}{2m_e}\frac{\alpha_{ne.le}^2}{r^2}\right) + \left(\frac{\hbar^2}{2m_h}\frac{\alpha_{nh.lh}^2}{r^2}\right) - \frac{1.8e^2}{2\varepsilon r}.$$

In the equation above, E_g is the bulk semiconductor band gap where the name originally appeared. The second and third terms, with $\alpha_{ne.le}^2$ and $\alpha_{nh.lh}^2$, are solutions (or "zeros") to the Bessel function for quantum numbers n and l, respectively, giving information about the electron/hole kinetic energy.

The Bessel function method solves the Schrodinger equation under initial spherical conditions and computes the kinetic energy of the electron/hole. Size dependency is related to kinetic energy via QD radius (r) in Bessel function solutions. m_e and m_h incorporate effective electron/hole masses. The approximation of the effective mass compensates for the periodic potential of the semiconductor lattice by changing a particle volume and considering it as a smooth particle. The final term (fourth term) is a first-order correction for the coulomb attraction between the electron and hole where e is the charge of an electron and ε is the dielectric constant of the material.

Two nanoparticle solution synthesis processes have been agreed upon the high and low temperature methods. The above growth rate equation can explain why the effects of the temperature differ from those of the calculation based on the total gas equation with monomer concentrations handled with vapor pressure [16].

$$C_r = C_\infty \exp\left(\frac{2\sigma}{nNK_BT}\right) \approx C_\infty\left(1 + \frac{2\sigma}{rNK_BT}\right),$$

$$C_x = C_\infty \exp\left(\frac{2\sigma}{r_cNK_BT}\right) \approx C_\infty\left(1 + \frac{2\sigma}{r_cNK_BT}\right),$$

where C_∞ is vapor pressure; C_r is the concentration of monomers at the nanocrystal surface; and C_x is the concentration of monomers far away from the crystal surface. The dependent growth rate temperature for crystal radius r is given by the following equation [16]

$$\frac{dr}{dt} = \frac{2\sigma\beta C_\infty}{N^2K_BT}\left(\frac{1}{r_c} - \frac{1}{r}\right), \quad (1)$$

where r_c is the critical radius at which the phase transition occurs; N is the number of atoms per unit volume; σ is the surface tension; β is the diffusion coefficient; K_B is the Boltzmann constan, and T is the temperature.

Based on the crystal radius r in Eq. (1), the word in parentheses defines whether a crystal has a positively or negatively increasing rate of size. When $r = r_c$, the crystalline phases are in equilibrium with zero crystal growth rate. When $r > r_c$, the crystal will grow. When $r < r_c$, the crystal will shrink. Ostwald ripening is a technique that aims to widen the size range of crystals while lowering the concentration of the resultant nanoparticles. Smaller crystals contract while bigger crystals develop. In Fig. 1, the form of Eq. (1) is shown. It is significant to remember that when $r = 2r_c$, the maximum growth rate may be calculated. The smaller crystals develop considerably quicker than the bigger crystals, and the average size is focused, resulting in a very narrow size distribution if the

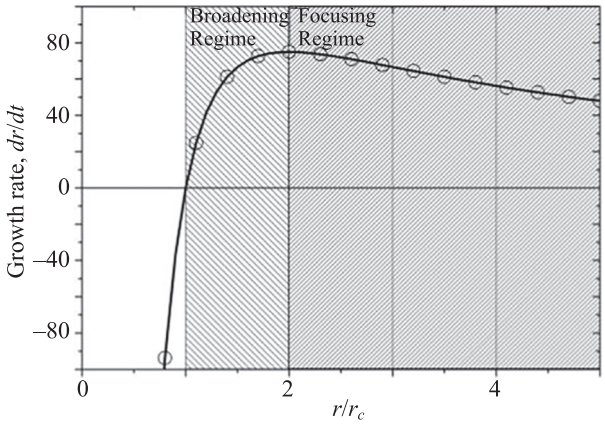

Fig. 1. An illustration form of the Eq. (1), illustrates the modes of size and dimension broadening specified by the average crystal radius $r_c < r < 2r_c$ and $r > 2r_c$, respectively [16]

entire size range is greater than this number. In reality, the typical technique repeatedly uses a monomer solution with a high enough concentration [17, 18].

Materials and Synthesis procedures

We developed a technique for producing isolated $AgInS_2$ nanoparticles with great size uniformity in an orthoxyle solution at high temperatures [19]. To boost luminous yield, we devised a method for synthesizing mixed $AgInS_2$ nanoparticles [20] which had a higher luminescence production than AgS or InS particles. The lattice period is also affected by changes in the Silver-to-Indium ratio. At a particular ratio, the structure varies from cubic for InS to hexagonal for AgS. Using diffuse transmission and reflection spectra, the kinetics of particle production and their characteristics were investigated. During synthesis durations up to 90 min, the solution absorption edge shifts to the short-wavelength area for diffuse transmission spectra. Following that, the edge gradually moves toward the long-wavelength region. As the contribution of the scattered signal is minimal in the region of significant absorption, the displacements are generated just by variations in the absorption of the solution components. One can explain the shift to the short-wavelength area by a sulfur drop which causes a large rise in the absorption coefficient in the 300–320 nm wavelength range. As the synthesis period rises, the size of the nanoparticles induces a shift to longer wavelengths. More complex behaviour is exhibited by reflection spectra. One might cause a simultaneous alteration in particle size, concentration, and refractive index of the medium. Techniques for manufacturing $AgInS_2$ nanoparticles at low and high temperatures were devised. The impact of the circumstances during synthesis on the formation and properties of nanoparticles was investigated. Depending on the concentration and according to an evaluation of the acquired absorption spectra of $AgInS_2$ nanoparticles, the location of the nanoparticles absorption edge shifts during the duration of the synthesis period for high-temperature synthesis. With an increase the ultrasonic action duration on the sample, the absorption edge in diffuse reflection spectra shifts by a short wavelength.

For $AgInS_2$ synthesis, with variations in solvent and temperature, portions of cold toluene were removed at various intervals and inputted for various Nano-Crystal (NC) sizes. The reaction mixture has a total volume of 30 ml. Base metal salt aqueous solution is: 0.71 ml of 0.1 M $InCl_3$; Thioglycolic Acid aqueous solution is: 0.6 ml of 1 M; concentrated ammonia is 0.3 ml; ammonium sulphide aqueous solution is: 0.174 ml of 2.9 M; 10 ml of 0.005 M silver nitrate aqueous solution was dripped in at a rate of 3 ml/hour. Following the NC synthesis, the ethanol cycle was centrifuged three times with toluene and then dissolved in toluene for storage. However, importantly, not the case that QDs may induce acute toxic effects, rather than that the aggregation of QD ions in key organs, as seen in vivo, might create significant chronic toxic consequences [21]. As seen in Fig. 2, *a*, *b*, we devised a revolutionary control technique by flashing a 405 nm laser on the solution during the synthesis and luminescence spectra were analyzed every 10s. Then the spectra were analyzed. A QE Pro spectrometer (Ocean Optics, USA), a 405 nm laser (200 mW), optical fibers, and filters are used in the experiment. Every ten seconds, the luminescence spectrum

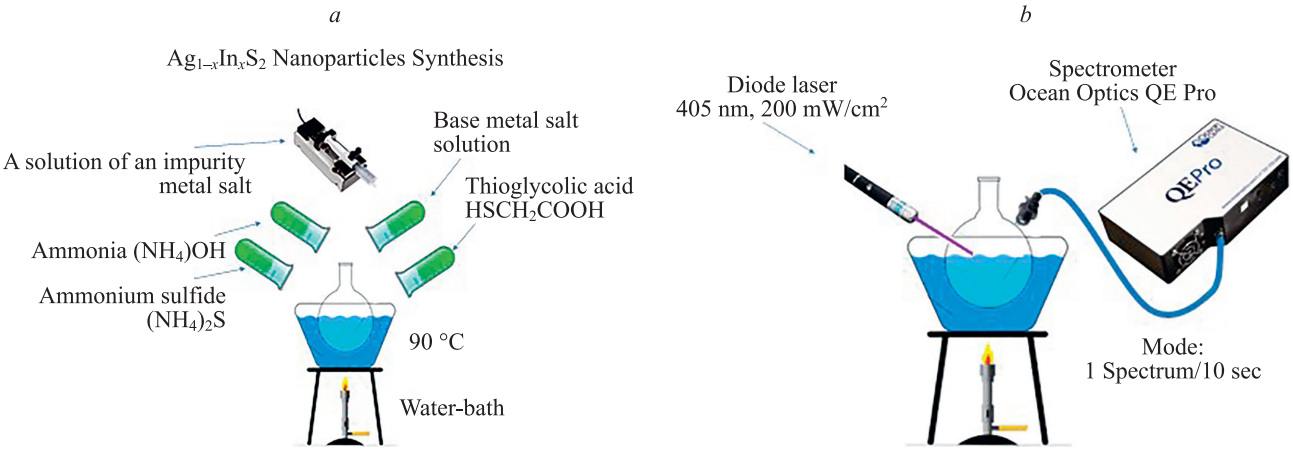

Fig. 2. Synthesis Control Methodology; $HSCH_2COOH$
a — aqueous nanoparticle synthesis, *b* — nanoparticle synthesis control method

of the reaction solution was recorded using a one-second laser stimulation.

Results and Discussions

The effects of the stoichiometric coefficient on the optical properties $Ag_xIn_{1-x}S_2$ nanoparticles, amplitude, wavelength of the peak of the luminescence band, and width of $AgInS_2$ nanoparticles are depicted in Fig. 3. The maximum luminescence wavelength moves to the IR region when the stoichiometric coefficient (x) changes. It is also worth noting that the amplitude begins to fall at a certain value.

The nanoparticles are identified by the altered InS structure induced by the presence of AgS impurities, according to X-ray analysis. Fig. 4 depicts the X-ray diffraction (XRD) spectra of doped QDs with various ratios of indium to silver (1:0.05, 1:0.1, 1:0.2, and 1:0.3). In general, relative intensity increases with an increase in silver ratio; nevertheless, there is no discernible shift in 2θ values. This shows that silver contributes to the diffraction of InAg/ZnS QDs doped with silver. The absence of a specific silver peak demonstrates the excellent incorporation of Ag_2S into the InAg matrix.

The X-ray fluorescence (XRF) patterns of $Ag_xIn_{1-x}S_2$ with different In concentrations (x: 0.03–0.18) and pure AgS are shown in Fig. 5. The structure is cubic in nature. Ag concentration is being increased.

According to our findings, one cane infers the temperature sensitivity of luminescence of $AgInS_2$ nanoparticles in terms of both the spectrum position and intensity of the luminescence maximum. The variation is caused by the energy states distortion of light and surface defects. In $Ag_xIn_{1-x}S_2$ samples, a transition in the structural phase from cubic to hexagonal and a temperature alteration change to a lower region occurs with an increase in Ag concentration.

Dynamic light scattering experiments were used to measure the average size of the received nanocrystals. The measurements were taken using a laser analyzer with a particle size of SZ100 (Horiba Jobin Yvon, Kyoto, Japan) and a measuring range for nanoparticle diameters ranging

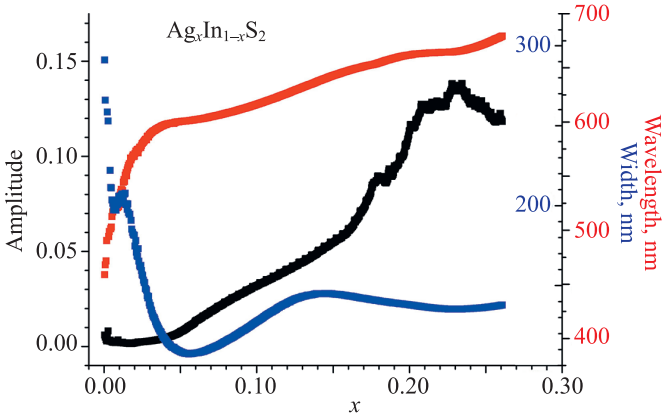

Fig. 3. Controlled synthesis of $Ag_xIn_{1-x}S_2$ nanoparticles. Illustrates the relation between the wavelength, the amplitude, and the width of $AgInS_2$ nanoparticles with the stoichiometric coefficient x

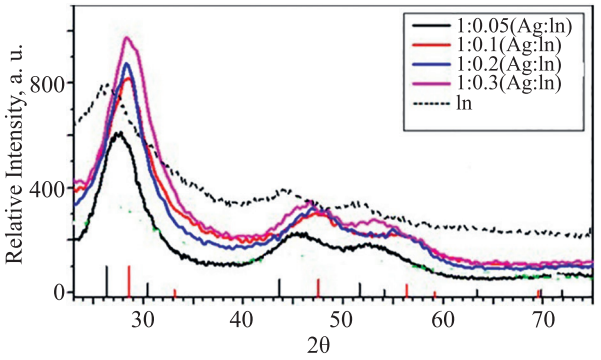

Fig. 4. XRD spectra of silver doped quantum dots with varying Ag:In ratios

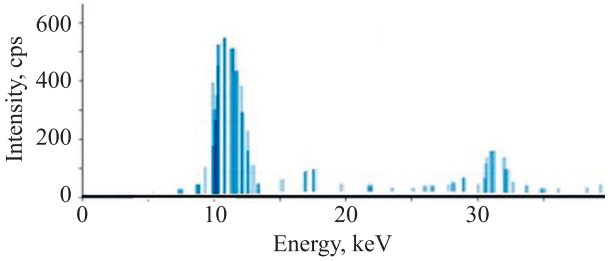

Fig. 5. Shown the $AgInS_2$ nanoparticles XRF analysis

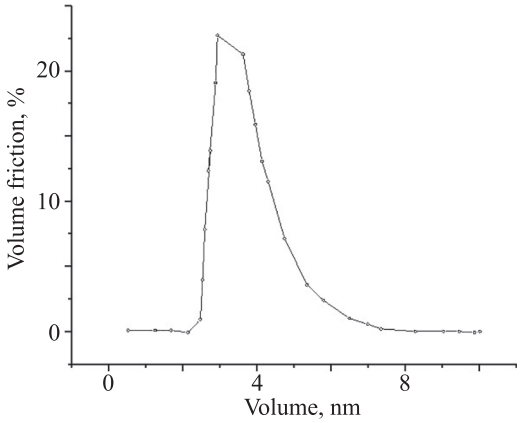

Fig. 6. The average particle size

from 0.3 nm to 8 nm. Forks have an average particle size of 3–3.5 nm (Fig. 6).

Conclusion

To increase luminescence yield, we devised a method for producing mixed $AgInS_2$ nanoparticles which have a higher luminescence yield than AgS or InS particles. When a certain ratio is reached, the arrangement of InS shifts to hexagonal for AgS. At lower substrate temperatures, the composition generates a hexagonal phase. As a result, it is now possible to change the orientation of a nanoparticle light band. The properties of mixed $AgInS_2$ nanoparticles for various production procedures, surface stability, and metal impurity introduction were examined. The link between the line width, maximum wavelength, luminescence amplitude, and the stoichiometric ratio is depicted in Fig. 3. It was

proven that adjusting the stoichiometric ratio of In and Ag in $Ag_xIn_{1-x}S_2$ nanoparticles does not allow for the maximum luminescence wavelength in biological tissue transparency. According to the data, from this it can be drawn that the synthesis of $Ag_xIn_{1-x}S_2$ nanoparticles (at x 0.25) does not permit the formation of nanoparticles with maximal luminescence band wavelengths greater than 800 nm. The amplitude of the luminescence bands decreases significantly as x exceeds 0.25. This change is caused by surface defects and distortion of the light energy levels. Nanoparticle agglomeration has no impact on the reported dependency.

References

1. Du W.M., Qian X.F., Yin J., Gong Q. Shape- and phase-controlled synthesis of monodisperse, single-crystalline ternary chalcogenide colloids through a convenient solution synthesis strategy. *Chemistry — A European Journal*, 2007, vol. 13, no. 31, pp. 8840–8846. https://doi.org/10.1002/chem.200700618
2. Ogawa T., Kuzuya T., Hamanaka Y., Sumiyama K.J. Synthesis of Ag–In binary sulfide nanoparticles—structural tuning and their photoluminescence properties. *Journal of Materials Chemistry*, 2010, vol. 20, no. 11, pp. 2226–2231. https://doi.org/10.1039/B920732E
3. Torimoto T., Adachi T., Okazaki K., Sakuraoka M., Shibayama T., Ohtani B., Kudo A., Kuwabata S. Facile synthesis of ZnS−AglnS$_2$ solid solution nanoparticles for a color-adjustable luminophore. *Journal of the American Chemical Society*, 2007, vol. 129, no. 41, pp. 12388–12389. https://doi.org/10.1021/ja0750470
4. Wang D.S., Zheng W., Hao C.H., Peng Q., Li Y. General synthesis of I–III–VI2 ternary semiconductor nanocrystals. *Chemical Communications*, 2008, vol. 22, pp. 2556–2558. https://doi.org/10.1039/B800726H
5. Xie R.G., Rutherford M., Peng X.G. Formation of high-quality I−III−VI semiconductor nanocrystals by tuning relative reactivity of cationic precursors. *Journal of the American Chemical Society*, 2009, vol. 131, no. 15, pp. 5691–5697. https://doi.org/10.1021/ja9005767
6. Feng Z.Y., Dai P.C., Ma X.C., Zhan J.H., Lin Z. Monodispersed cation-disordered cubic $AgInS_2$ nanocrystals with enhanced fluorescence. *Applied Physics Letters*, 2010, vol. 96, no. 1, pp. 013104. https://doi.org/10.1063/1.3280372
7. Chopra K.L., Das S.R. *Thin Film Solar Cells*. New York; London, 1983.
8. Alkhasov A.B. *Renewable Energy*. Moscow, Fizmatlit Publ., 2010. 255 p. (in Russian)
9. Ariezo M., Loferski J.J. Investigation of potentially high efficiency photovoltaic cells consisting of two heterojunctions on a common wide band gap semiconductor base. *Proc. of the 13th IEEE Photovoltaic Specialists Conference*, 1978, pp. 898–903.
10. Abdullaev M.A., Alhasov A.B., Magomedova D.Kh. Fabrication and properties of $CuInSe_2$/$AgInSe_2$/CdS double heterojunction cascade solar cells. *Inorganic Materials*, 2014, vol. 50, no. 3, pp. 228–232. https://doi.org/10.1134/S0020168514030017
11. Maestro L.M., Rodríguez E.M., Rodríguez F.S., Iglesias-de la Cruz M.C., Juarranz A., Naccache R., Vetrone F., Jaque D., Capobianco J.A., Solé J.G. CdSe quantum dots for two-photon fluorescence thermal imaging. *Nano Letters*, 2010, vol. 10, no. 12, pp. 5109–5115. https://doi.org/10.1021/nl1036098
12. Yang J.M., Yang H., Lin L. Quantum dot nano thermometers reveal heterogeneous local thermogenesis in living cells. *ACS Nano*, 2011, vol. 5, no. 6, pp. 5067–5071. https://doi.org/10.1021/nn201142f
13. Skaptsov A.A., Ustalkov S.O., Mohammed A.H., Savenko O.A., Novikova A.S., Kozlova E.A., Kochubey V.I. Fabrication and characterization of biological tissue phantoms with embedded nanoparticles. *Journal of Physics: Conference Series*, 2017, vol. 917, no. 4, pp. 042003. https://doi.org/10.1088/1742-6596/917/4/042003
14. Ustalkov S.O., Kozlova E.A., Savenko O.A., Mohammed A.H., Kochubey V.I., Skaptsov A.A. Influence of excitation power density on temperature dependencies of $NAYF_4$:Yb, Er nanoparticles luminescence spectra. *Proceedings of SPIE*, 2017, vol. 10336, pp. 1033614. https://doi.org/10.1117/12.2269297
15. Jensen R.A. *Optical studies of colloidal quantum dots: optical trapping with plasmonic nano apertures and thermal recovery from photoinduced dimming. PhD thesis*. Department of Chemistry, Massachusetts Institute of Technology, 2015.
16. Booth M. *Synthesis and characterisation of $CuInS_2$ quantum dots. PhD thesis*. The University of Leeds School of Physics & Astronomy, 2014.

Литература

1. Du W.M., Qian X.F., Yin J., Gong Q. Shape- and phase-controlled synthesis of monodisperse, single-crystalline ternary chalcogenide colloids through a convenient solution synthesis strategy // Chemistry — A European Journal. 2007. V. 13. N 31. P. 8840–8846. https://doi.org/10.1002/chem.200700618
2. Ogawa T., Kuzuya T., Hamanaka Y., Sumiyama K.J. Synthesis of Ag–In binary sulfide nanoparticles—structural tuning and their photoluminescence properties // Journal of Materials Chemistry. 2010. V. 20. N 11. P. 2226–2231. https://doi.org/10.1039/B920732E
3. Torimoto T., Adachi T., Okazaki K., Sakuraoka M., Shibayama T., Ohtani B., Kudo A., Kuwabata S. Facile synthesis of ZnS−$AgInS_2$ solid solution nanoparticles for a color-adjustable luminophore // Journal of the American Chemical Society. 2007. V. 129. N 41. P. 12388–12389. https://doi.org/10.1021/ja0750470
4. Wang D.S., Zheng W., Hao C.H., Peng Q., Li Y. General synthesis of I–III–VI2 ternary semiconductor nanocrystals // Chemical Communications. 2008. V. 22. P. 2556–2558. https://doi.org/10.1039/B800726H
5. Xie R.G., Rutherford M., Peng X.G. Formation of high-quality I−III−VI semiconductor nanocrystals by tuning relative reactivity of cationic precursors // Journal of the American Chemical Society. 2009. V. 131. N 15. P. 5691–5697. https://doi.org/10.1021/ja9005767
6. Feng Z.Y., Dai P.C., Ma X.C., Zhan J.H., Lin Z. Monodispersed cation-disordered cubic $AgInS_2$ nanocrystals with enhanced fluorescence // Applied Physics Letters. 2010. V. 96. N 1. P. 013104. https://doi.org/10.1063/1.3280372
7. Чопра К.Л., Дас С.Р. Тонкопленочные солнечные элементы. М.: Мир, 1986. 440 с.
8. Алхасов А.Б. Возобновляемая энергетика. М.: Физматлит, 2010. 255 с
9. Ariezo M., Loferski J.J. Investigation of potentially high efficiency photovoltaic cells consisting of two heterojunctions on a common wide band gap semiconductor base // Proc. of the 13th IEEE Photovoltaic Specialists Conference. 1978. P. 898–903.
10. Abdullaev M.A., Alhasov A.B., Magomedova D.Kh. Fabrication and properties of $CuInSe_2$/$AgInSe_2$/CdS double heterojunction cascade solar cells // Inorganic Materials. 2014. V. 50. N 3. P. 228–232. https://doi.org/10.1134/S0020168514030017
11. Maestro L.M., Rodríguez E.M., Rodríguez F.S., Iglesias-de la Cruz M.C., Juarranz A., Naccache R., Vetrone F., Jaque D., Capobianco J.A., Solé J.G. CdSe quantum dots for two-photon fluorescence thermal imaging // Nano Letters. 2010. V. 10. N 12. P. 5109–5115. https://doi.org/10.1021/nl1036098
12. Yang J.M., Yang H., Lin L. Quantum dot nano thermometers reveal heterogeneous local thermogenesis in living cells // ACS Nano. 2011. V. 5. N 6. P. 5067–5071. https://doi.org/10.1021/nn201142f
13. Skaptsov A.A., Ustalkov S.O., Mohammed A.H., Savenko O.A., Novikova A.S., Kozlova E.A., Kochubey V.I. Fabrication and characterization of biological tissue phantoms with embedded nanoparticles // Journal of Physics: Conference Series. 2017. V. 917. N 4. P. 042003. https://doi.org/10.1088/1742-6596/917/4/042003
14. Ustalkov S.O., Kozlova E.A., Savenko O.A., Mohammed A.H., Kochubey V.I., Skaptsov A.A. Influence of excitation power density on temperature dependencies of $NAYF_4$:Yb, Er nanoparticles luminescence spectra // Proceedings of SPIE. 2017. V. 10336. P. 1033614. https://doi.org/10.1117/12.2269297
15. Jensen R.A. Optical studies of colloidal quantum dots: optical trapping with plasmonic nano apertures and thermal recovery from photoinduced dimming: PhD thesis. Department of Chemistry, Massachusetts Institute of Technology, 2015.
16. Booth M. Synthesis and characterisation of $CuInS_2$ quantum dots: PhD thesis. The University of Leeds School of Physics & Astronomy, 2014.

17. Peng X., Wickham J., Alivisatos A.P. Kinetics of II-VI and III-V colloidal semiconductor nanocrystal growth: “focusing” of size distributions. *Journal of the American Chemical Society*, 1998, vol. 120, no. 21, pp. 5343–5344. https://doi.org/10.1021/ja9805425
18. Mohmmed A.H., Skaptsov A.A., Ahmad A.K. Luminescence method to characterize the synthesis of ZnCdS quantum dots in real time. *Materials Today: Proceedings*, 2021, vol. 42, pp. 2803–2807. https://doi.org/10.1016/j.matpr.2020.12.725
19. Kochubey V.I., Konyukhova Ju.G., Volkova E.K. Effect of polyacrylic acid shell on luminescence and phosphorescence of ZnCdS nanoparticles. *Book of Abstracts of the 3rd International Symposium “Molecular photonics”*, St. Petersburg, Russia, VVM Publishing Ltd, 2012, pp. 137.
20. Volkova E.K., Kochubeĭ V.I. Synthesis and luminescent characteristics of CdS nanoparticles. *International Symposium «Nanophotonics-2011»: Collection of the reports abstracts and programs*. Ukraine, Crimea, 2011, pp. 1–2. (in Russian)
21. Volkova E.K., Yanina I.Yu., Sagaydachnaya E., Konyukhova J.G., Kochubey V.I., Tuchin V.V. Effect of luminescence transport through adipose tissue on measurement of tissue temperature bY using ZnCdS nanothermometers. *Proceedings of SPIE*, 2018, vol. 10493, pp. 104931K. https://doi.org/10.1117/12.2295620

17. Peng X., Wickham J., Alivisatos A.P. Kinetics of II-VI and III-V colloidal semiconductor nanocrystal growth: “focusing” of size distributions // Journal of the American Chemical Society. 1998. V. 120. N 21. P. 5343–5344. https://doi.org/10.1021/ja9805425
18. Mohmmed A.H., Skaptsov A.A., Ahmad A.K. Luminescence method to characterize the synthesis of ZnCdS quantum dots in real time // Materials Today: Proceedings. 2021. V. 42. P. 2803–2807. https://doi.org/10.1016/j.matpr.2020.12.725
19. Kochubey V.I., Konyukhova Ju.G., Volkova E.K. Effect of polyacrylic acid shell on luminescence and phosphorescence of ZnCdS nanoparticles // Book of Abstracts of the 3rd International Symposium “Molecular photonics”. St. Petersburg, Russia: VVM Publishing Ltd, 2012. P. 137.
20. Волкова Е.К., Кочубей В.И. Синтез и люминесцентные характеристики наночастиц CdS // Международный симпозиум «Нанофотоника-2011»: сборник тезисов докладов и программ. Украина, Крым. 2011. С. 1–2.
21. Volkova E.K., Yanina I.Yu., Sagaydachnaya E., Konyukhova J.G., Kochubey V.I., Tuchin V.V. Effect of luminescence transport through adipose tissue on measurement of tissue temperature bY using ZnCdS nanothermometers // Proceedings of SPIE. 2018. V. 10493. P. 104931K. https://doi.org/10.1117/12.2295620

Authors

Ahmad K. Ahmad — PhD, Full Professor, Al-Nahrain University, College of Engineering, Baghdad, 10072, Iraq, SC 56756921400, https://orcid.org/0000-0003-3522-4701, Ahmad.ahmad@nahrainuniv.edu.iq

Ammar H. Mohammed — PhD, Lecturer, Al-Nahrain University, College of Science, Baghdad, 10072, Iraq, SC 57191197465, https://orcid.org/0000-0003-3646-4790, ammarhussen659@gmail.com

Alexander A. Skaptsov — PhD (Physics & Mathematics), Associate Professor, Saratov State University, Saratov, 410012, Russian Federation, SC 22951907500, https://orcid.org/0000-0001-9336-6885, skaptsov@yandex.ru

Авторы

Ахмад Ахмад Карнал — PhD, профессор, профессор, Аль-Нарейн Юниверсити, Инженерный колледж, Багдад, 10072, Ирак, SC 56756921400, https://orcid.org/0000-0003-3522-4701, ahmad.ahmad@nahrainuniv.edu.iq

Мохаммед Аммар Хуссейн — PhD, преподаватель, Аль-Нарейн Юниверсити, Багдад, 10072, Ирак, SC 57191197465, https://orcid.org/0000-0003-3646-4790, ammarhussen659@gmail.com

Скапцов Александр Александрович — кандидат физико-математических наук, доцент, Саратовский национальный исследовательский государственный университет имени Н.Г. Чернышевского, Саратов, 410012, Российская Федерация, SC 22951907500, https://orcid.org/0000-0001-9336-6885, skaptsov@yandex.ru

Received 29.07.2022
Approved after reviewing 09.09.2022
Accepted 09.11.2022

Статья поступила в редакцию 29.07.2022
Одобрена после рецензирования 09.09.2022
Принята к печати 09.11.2022